

Gas transport properties of highly fluorinated polyamideimides

Z.-K. Xu*, M. Böhning and J. Springer†

Technische Universität Berlin, Institute für Technische Chemie, Straße des 17. Juni 135, 10623 Berlin, Germany

and N. Steinhauser and R. Mülhaupt

Freiburger Materialforschungszentrum and Institut für Makromolekulare Chemie, Stefan-Meier-Straße 31, 79106 Freiburg i. Br., Germany

(Received 29 September 1995; revised 11 March 1996)

Gas transport properties of a series highly fluorinated polyamideimides based on 2,2-bis(3,4-decarboxy-phenyl)hexafluoropropane dianhydride and *N,N*-bis(amino-phenyl)-perfluoroalkane- α,ω -dicarboxamide diamines have been measured as a function of upstream pressure and temperature. The results show that the permeability coefficients P for the penetrant gases in any of the four polyamideimides decrease in the gas order: $P(\text{CO}_2) > P(\text{O}_2) > P(\text{N}_2) > P(\text{CH}_4)$, while the permeabilities for a given gas in these polymers increase with the increase of oligo(tetrafluoroethene) segment length. The effects of the substitution pattern of the phenyl ring and the length of the oligo(tetrafluoroethene) segments in the diamine moieties on gas permeabilities, diffusivities and solubilities are discussed. It seems that, comparing with the effect of the flexible oligo(tetrafluoroethene) segment, the substitution patterns of phenyl group in the diamine moieties have no notable effect of the diffusivities in the polyamideimides as the length of the oligo(tetrafluoroethene) segment increasing from 8 to 12 carbons. The activation energies of permeation and diffusion were obtained for the gas/polymer pairs studied and correlated with the size of penetrant gas. © 1997 Elsevier Science Ltd. All rights reserved.

(Keywords: gas permeation; highly-fluorinated polyamideimides; oligo(tetrafluoroethane))

INTRODUCTION

Gas separation by selective permeation through polymeric membranes is one of the fastest growing branches of separation technology^{1,2}. Strong interest exists in the synthesis of new polymers that exhibit both higher gas permeabilities and higher selectivities than presently available polymers. Such new polymers are required in order to reduce the cost of extant membrane processes for gas separation. To develop good membrane materials combining both high permeabilities and high selectivities, it is essential to investigate systematically the relationships between the chemical and physical structures of the polymers and their gas permeabilities. However, it is only in recent years that the relationship of structure, permeability and selectivity of polymers has become the object of many systematic studies^{3–21}. Based on these systematic investigations, several criteria have been proposed for polymer structures that might exhibit a high gas permeability as well as a high selectivity. The acquirement and the application of these criteria have led to the development of high transition temperature amorphous polymers, such as polycarbonates^{3,4},

polysulfones^{5,6} and polyimides^{7–22}, as the new generation of gas separation membrane materials. Among these high performance polymers, polyimides with excellent thermal and mechanical durability have attracted much attention^{7–22}. Recently, it was reported that polyimides with 2,2-bis(3,4-decarboxyphenyl)-hexafluoro-propane dianhydride (6FDA) show both a higher gas permeability and a higher gas selectivity than do the general polyimides and the conventional polymers^{14–22}. The primary objective of our series of studies^{22,23} is to combine the typical properties of 6FDA-based polyimides with the properties of other polymers, such as polysulfone and poly(1,4-phenylene sulfide)^{24–28}. In the present work, the gas transport properties of four highly-fluorinated 6FDA-based polyamideimides containing an oligo(tetrafluoroethene) segment in the polymer chain were studied. Fluoropolymers such as poly(tetrafluoroethene) are well known to exhibit unusual properties, e.g. high thermal and environmental stabilities, high abrasion resistance, low water-uptake with hydrophobic and oleophobic surface. Moreover, perfluorinated polymers usually show rather high solubilities for CO₂ and O₂.

BACKGROUND

The permeability of a flat polymer membrane is given by equation (1) as the steady state flux per unit area (J_s)

* Permanent address: Department of Polymer Science & Engineering, Zhejiang University, 310027 Hangzhou, P. R. China

† To whom correspondence should be addressed

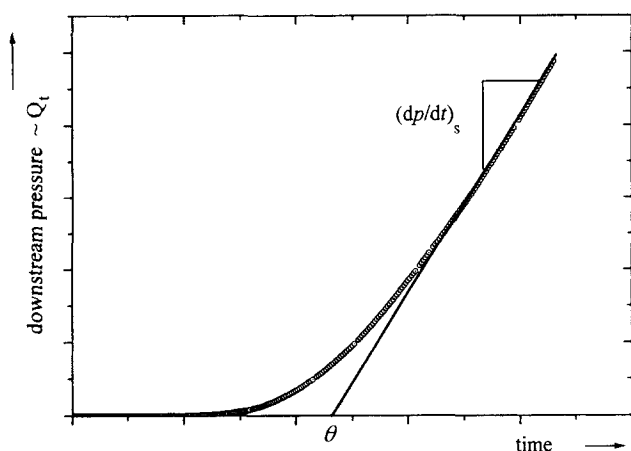


Figure 1 Typical curve of the total amount of permeated pentrant (Q_t) vs time during a transient permeation experiment under time-lag boundary conditions

normalized by the pressure difference across the membrane cross-section ($p_2 - p_1$) and the membrane thickness (l)²⁹.

$$P = J_s \cdot \frac{l}{p_2 - p_1} \quad (1)$$

From a single transient gas transport experiment both the permeability coefficient (P) and the diffusion coefficient (D) can be obtained. Usually the time-lag boundary conditions are employed for such measurements, i.e. the membrane is initially degassed and upstream pressure (p_2) as well as downstream pressure ($p_1 = 0$) are held constant during the whole experiment.

Figure 1 shows the typical course of the total amount of permeated pentrant (Q_t) vs time for such a permeation measurement. The transient part of the permeation curve can be characterized by the time-lag θ , obtained by extrapolation of the steady state part of the curve to the time axis, and an effective diffusion coefficient (D_{eff}) can be calculated according to equation (2)²⁹.

$$D_{\text{eff}} = \frac{l^2}{6\theta} \quad (2)$$

In the case of glassy polymer membranes the diffusion coefficient calculated according to equation (2) can deviate from the 'true' diffusion coefficient due to the non-equilibrium state of the material and the slow response to the presence of a penetrant concentration gradient³⁰. Therefore it is also often referred to as apparent diffusion coefficient D_{app} . Nevertheless D_{eff} gives a good estimation of the diffusion behaviour of gases in polymer materials. The permeability coefficient is calculated from the slope of the linear part of the curve representing the steady state flux J_s .

Ideal permselectivities

Ideal permselectivities $\alpha_{A/B}$ determined from individual pure gas permeability measurements of gases A and B (P_A , P_B) according to equation (3) are often considered to be useful in order to estimate the separation characteristics of a membrane material.

$$\alpha_{A/B} = \frac{P_A}{P_B} \quad (3)$$

Within this simplified view it has to be taken into account that in real gas mixtures gas/gas and gas/polymer interactions as well as competition with respect to sorption and diffusion processes may occur and lead to deviations from the ideal behaviour. In spite of this fact ideal permselectivities are often used as a first measure of the separation potential of new polymer materials for dense gas separation membranes.

Generally the permeation of small penetrants through nonporous polymer membranes is described in terms of a solution-diffusion process, i.e. the permeation is a combination of the fundamental processes of sorption (solution) at the membrane upstream surface and diffusion through the polymer matrix. The desorption of the sorbed penetrant molecules at the downstream side can be neglected regarding the description of the overall transport process³¹. Therefore the permeability can be described as the product of diffusivity (D) and solubility (S) of the penetrant gas in the polymeric membrane material (equation (4)).

$$P = D \cdot S \quad (4)$$

To better understand the gas permeabilities, it is useful to separate the permeability coefficient into its kinetic and thermodynamic components D and S , respectively. Although the applicability of equation (4) to glassy polymers is limited due to the non-equilibrium nature of the glassy state, the calculation of solubility data based on time-lag measurements allows a more detailed discussion of the transport properties, at least in a qualitative way. Furthermore, the ideal overall permselectivity (equation (3)) can also be factored into diffusivity ($\alpha_{A/B}^D$) and solubility ($\alpha_{A/B}^S$) terms using equation (4) to give:

$$\alpha_{A/B} = \alpha_{A/B}^D \cdot \alpha_{A/B}^S = \frac{D_A}{D_B} \cdot \frac{S_A}{S_B} \quad (5)$$

Temperature dependence of transport properties

Within a temperature range in which no significant thermal transitions of the polymer occur, the temperature dependence of permeability and diffusivity can be described by two Arrhenius expressions³²:

$$P = P_0 \cdot \exp\left(-\frac{E_P}{RT}\right) \quad (6)$$

$$D = D_0 \cdot \exp\left(-\frac{E_D}{RT}\right) \quad (7)$$

where P_0 and D_0 are pre-exponential factors, E_D is the activation energy of diffusion, E_P is the apparent activation energy of permeation, resulting according to equation (4) as the sum of E_D and the heat of sorption ΔH_S . R is the universal gas constant and T is the temperature. These relations can be used as a convenient method to calculate permeabilities and diffusivities at different temperatures within the range of validity. On the other hand the obtained parameters may also provide a better insight into the basic processes involved in gas permeability.

Units

The transport parameters determined within this study are given in the widely accepted and usually employed units. The permeability coefficient P is given in Barrers,

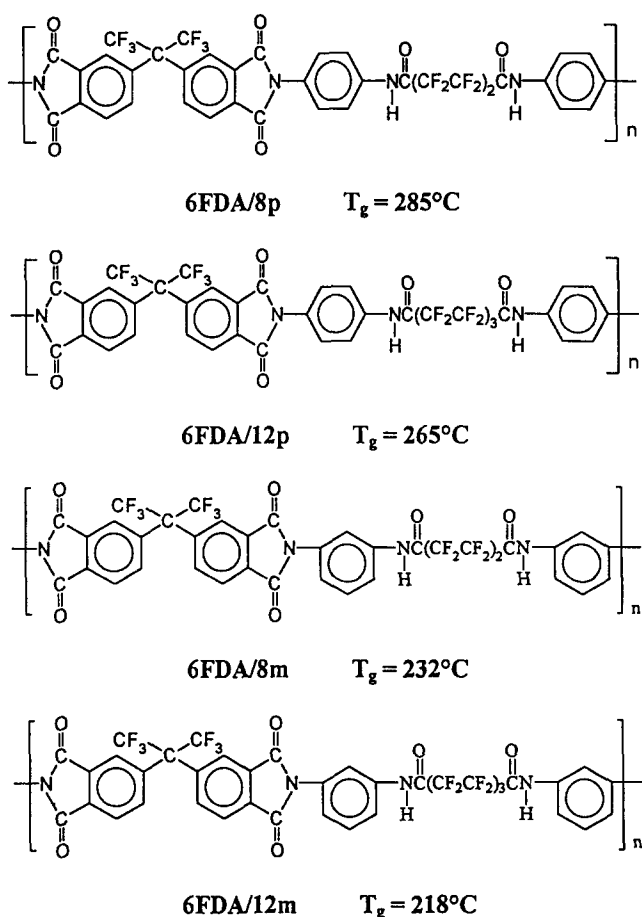


Figure 2 Molecular structure and T_g of 6FDA-polyamideimides studied

where 1 Barrer = $10^{-10} \text{cm}^3(\text{STP})/\text{cm}^2\text{cmHg}$, while the diffusion coefficient D (D_{eff}) is given in cm^2/s and the solubility coefficient in $\text{cm}^3(\text{STP})/\text{cm}^3\text{atm}$.

EXPERIMENTAL

Materials

Four different 6FDA-based polyamideimides were synthesized from 6FDA and *N,N*-bis(aminophenyl)-perfluoroalkane- α,ω -dicarboxamide diamines by methods reported in a previous paper²³. The chemical structures, designations and glass transition temperatures (T_g s) of the polymers under investigation are shown in Figure 2. The T_g s were determined using a Rheometric Solid Analyser RSA II at a heating rate of $10^\circ\text{C min}^{-1}$ and an oscillation frequency of 1 Hz.

Carbon dioxide, oxygen, nitrogen, and methane were obtained from Messer Griesheim GmbH. The purity of CH_4 was stated by the supplier to be 99.5% or better, the other gases had purities $>99.99\%$. The gases were used without further purification.

Membrane preparation

The polymers were used in the form of nonporous planar membranes which were prepared by casting DMF solutions containing 20 wt% polymer onto glass plates and dried for 24 h at 100°C in a vacuum oven. After removing from the glass plates the membranes were dried for another 24 h at 100°C under vacuum. All membranes were treated according to the same procedure and the

resulting thicknesses ranged from 20 to $40 \mu\text{m}$. The individual membrane thickness, used for the calculation of permeability and diffusivity, was determined as a mean value from at least five single measurements within the whole membrane area using a digital Mitutoyo gauge providing a resolution of $1 \mu\text{m}$. Homogeneity concerning the membrane thickness was always better than $\pm 5\%$.

Apparatus and experimental procedure

The gas transport measurements presented in this study were performed at penetrant pressures ranging from 1 to 20 atm at 35°C and at 10 atm at temperatures between 25 and 45°C , respectively. Permeability coefficients P as well as effective diffusion coefficients D_{eff} (for the sake of simplicity further referred to as D) were measured according to the time-lag method using an experimental set-up developed in our laboratory^{27,28,33}. The dense membrane was placed in a permeation cell, sealed between two O-rings and mechanically supported by a highly porous metal plate. On the downstream side a constant volume, separated by a high vacuum valve, with a precision capacitance pressure gauge MKS Baratron 128A, is attached to the cell. On the upstream side an autoclave allows the pre-adjustment of the penetrant pressure. All parts are held at a constant temperature ($\pm 0.2^\circ\text{C}$) in an air bath inside a thermostatted housing. The temperature of the Baratron gauge, providing a resolution of $1 \mu\text{bar}$ corresponding to 0.01% of the full scale (10 mbar), is controlled at 100°C in order to minimize effects of ambient or penetrant temperature variations.

Prior to the measurement the membrane is degassed in vacuum within the permeation cell for at least 5 h using an oil diffusion pump in connection with a rotary oil pump. To start the measurement the upstream side of the membrane is exposed instantaneously to the pre-adjusted penetrant pressure while the pressure increase in the constant downstream volume, caused by the permeate flux through the membrane, is monitored. Deviations from the time-lag boundary conditions can be neglected since $p_2 \ll p_1$ and $p_2 \approx 0$. The time dependent downstream pressure signal, proportional to the total amount of permeated penetrant, is registered together with the upstream pressure (piezoresistive gauge) and the cell temperature (Pt100 thermoresistor) by means of a desktop personal computer. The resulting data set is then analysed by performing a linear regression on the linear part of the downstream pressure curve. The error for the absolute values of the permeability coefficients can be estimated to about $\pm 10\%$, due to uncertainties of the determination of the downstream volume and the effective membrane area and thickness, while the reproducibility is better than $\pm 4\%$.

Activation energies and pre-exponential factors were determined by plotting the temperature dependent data in Arrhenius coordinates and performing a linear regression analysis.

RESULTS AND DISCUSSION

Gas permeabilities and permselectivities of the 6FDA-based polyamideimides

The effect of upstream pressure on the pure gas permeability coefficients at 35°C is shown in Figures 3 and 4 for the four polyamideimides studied. Each of

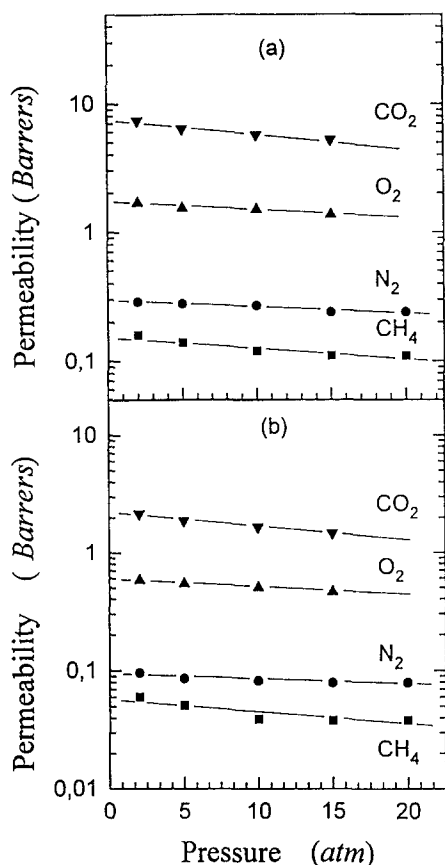


Figure 3 Effect of pressure on the gas permeability coefficients of (a) 6FDA/8p and (b) 6FDA/8m polyamideimides at 35°C

these figures presents values of P for CO_2 , O_2 , N_2 and CH_4 for a given pair of *para* and *meta* isomers of the polyamideimides. The straight lines in the figures were obtained from least-squares regressions of the experimental data. Over the pressure range covered here, none of the polymers exhibits gas-induced plasticization, which would be signalled by an increase in permeability with increasing upstream pressure. Resistance to plasticization is an important property of membrane materials, particularly in high-pressure applications such as CO_2 stripping from the natural gas stream, since plasticized polymers usually exhibit markedly reduced selectivities to penetrant gas mixtures.

It can be seen from *Figures 3* and *4* that the values of P are either approximately independent of the upstream pressure or decrease slightly with increasing the pressure between the interval of 1 to 20 atm. These results are consistent with the results of other studies^{9,20–21}. The decrease of P with increasing gas pressure observed in some cases for N_2 and CH_4 is probably also influenced by larger experimental errors at low pressures, because of the low permeation rates of these gases under these pressure conditions. *Figures 3* and *4* also show that the permeability coefficients of the 6FDA-based polyamideimides decrease in the gases order

$$\text{CO}_2 > \text{O}_2 > \text{N}_2 > \text{CH}_4$$

just in accordance with the order of increasing 'kinetic' diameters (σ_k) of the penetrant molecules³⁴, calculated from the minimum equilibrium cross-sectional diameter. The permeability data measured at 10 atm and 35°C are summarized in *Table 1*. This table shows that the

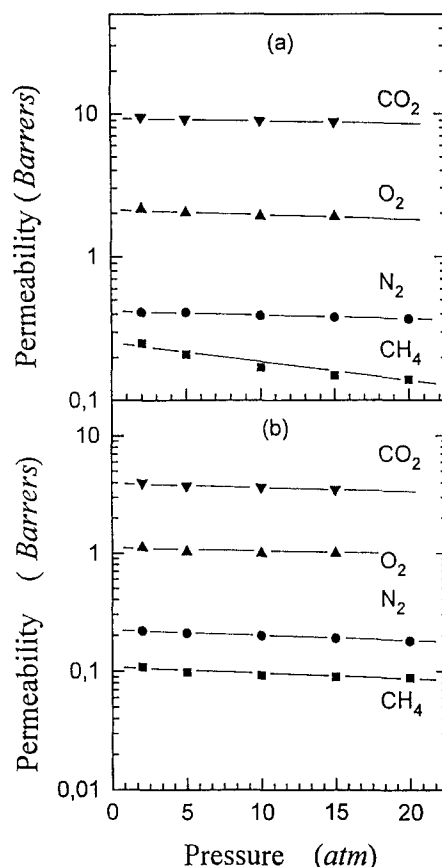


Figure 4 Effect of pressure on the gas permeability coefficients of (a) 6FDA/12p and (b) 6FDA/12m polyamideimides at 35°C

Table 1 Permeabilities^a and permselectivities for CO_2 , O_2 , N_2 , and CH_4 in four 6FDA-polyamideimides at 35°C and 10 atm

Polymer	P_{CO_2}	P_{CH_4}	$\alpha_{\text{CO}_2/\text{CH}_4}$	P_{O_2}	P_{N_2}	$\alpha_{\text{O}_2/\text{N}_2}$
6FDA/8p	5.72	0.12	47.7	1.49	0.27	5.52
6FDA/8m	1.66	0.04	41.6	0.49	0.08	6.12
6FDA/12p	8.91	0.17	52.4	1.90	0.39	4.87
6FDA/12m	3.64	0.09	40.4	1.00	0.20	5.00

^a Barrers ($10^{-10} \text{ cm}^3 (\text{STP}) \text{ cm}^{-2} \text{ s}^{-1} \text{ cmHg}^{-1}$)

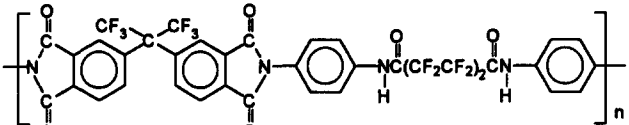
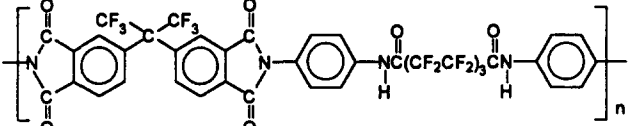
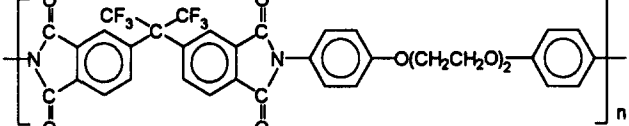
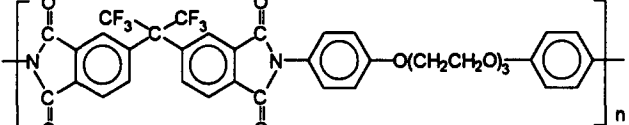
permeability coefficients for a given gas in the four 6FDA-polyamideimides with oligo(tetrafluoroethene) in the diamine moieties decrease in the polymer order:

$$6\text{FDA}/12\text{p} > 6\text{FDA}/8\text{p} > 6\text{FDA}/12\text{m} > 6\text{FDA}/8\text{m}$$

These results indicate that the gas transport properties in the highly-fluorinated 6FDA-polyamideimides studied here are primarily affected by the substitution pattern of the phenyl ring in the *N,N*-bis(aminophenyl)-perfluoroalkane- α, ω -dicarboxamide diamine components and the length of the oligo(tetrafluoroethene) segment (or fluorine content) in these diamine moieties.

Regardless of the length of the oligo(tetrafluoroethene) in the diamine moieties, the two *para*-connected polymers show higher gas permeabilities for all gases and a higher permselectivity towards the CO_2/CH_4 system compared to their *meta* isomers. As can be seen from *Table 1*, the permeability coefficient of CO_2 in 6FDA/12p is 5.4 and 2.4 times larger than in 6FDA/8m and 6FDA/12m, respectively, while the permselectivity of CO_2/CH_4 system in the former polyamideimide is about 26% and 30% higher than those of 6FDA/8m and 6FDA/12m.

Table 2 Comparison of structurally related polymers

Polymer structure	T_g (°C)	P_{CO_2} (Barrers)	α_{CO_2/CH_4}	P_{O_2} (Barrers)	α_{O_2/N_2}	Ref.
	285	5.72	48.9	1.49	5.52	This study ^a
	265	8.91	53.4	1.90	5.00	This study
	195	2.50	34.3	0.50	5.14	21 ^b
	157	1.94	43.3	0.33	4.85	21

^a Data at 35°C and 10 atm^b Data at 35°C and 6.8 atmTable 3 Diffusion coefficients^d and diffusion selectivities at 35°C and 10 atm

Polymer	D_{CO_2}	D_{CH_4}	α_{CO_2/CH_4}^D	D_{O_2}	D_{N_2}	α_{O_2/N_2}^D
6FDA/8p	0.95	0.07	13.6	1.64	0.39	4.20
6FDA/8m	0.47	0.04	11.8	1.03	0.34	3.03
6FDA/12p	1.16	0.10	11.5	2.26	0.43	5.26
6FDA/12m	1.00	0.11	9.10	2.11	0.53	3.98

^d $10^{-8} \text{cm}^2 \text{s}^{-1}$ Table 4 Solubility coefficients^d and solubility selectivities at 35°C and 10 atm

Polymer	S_{CO_2}	S_{CH_4}	α_{CO_2/CH_4}^S	S_{O_2}	S_{N_2}	α_{O_2/N_2}^S
6FDA/8p	4.58	1.30	3.51	0.69	0.53	1.31
6FDA/8m	2.68	0.80	3.36	0.36	0.18	1.98
6FDA/12p	5.84	1.29	4.52	0.64	0.56	1.14
6FDA/12m	2.77	0.64	4.31	0.36	0.29	1.25

^d $\text{cm}^3(\text{STP}) \text{cm}^{-3}(\text{polymer}) \text{atm}^{-1}$

Recent investigations have shown that the *para*-connected polymers commonly exhibit a higher gas permeability and a lower selectivity than their corresponding *meta* isomers for a variety of polymers including polyimides^{9,10,12,14,16}, polysulfones⁶, polyesters³⁵ and poly(phenolphthalein phthalates)³⁶. It has been suggested by Stern *et al.*⁹ and other authors^{12,14} that phenyl rings connected to adjacent moieties at a *para* position can rotate around their principle axis, thereby increasing the free volume of the polymer, in turn, the gas permeabilities. However, the phenyl rings connected at a *meta* position cannot rotate without cooperative motion of the neighbouring moieties. In the glassy state, the local mobility of a *meta*-linked phenyl ring is restricted. This speculation has been confirmed by Mi *et al.*¹⁰ in accordance with dynamic mechanical analysis and theoretical calculations of the torsional energies for the rotation of a single bond in pyromellitic

dianhydride/3,3'-oxydianiline (PMDA-3,3'-ODA) and pyromellitic dianhydride/4,4'-oxydianiline (PMDA-4,4'-ODA) polyimides. Furthermore, this hypothesis is also consistent with the view suggested by Pavlova *et al.*³⁷ through calculating conformational parameters with the Monte-Carlo simulation. According to that, the rotation about a bond passing through the phenyl ring is forbidden if this virtual bond and valence bond joined to the phenyl ring do not lie on a straight line. However, the higher CO_2/CH_4 permselectivity of the *para*-connected polyamideimides relative to their *meta* isomers as revealed by this study is unexpected. The reason for this anomaly is unclear at present. As with all other polyimides reported by Stern *et al.*²¹ and in our previous paper²², the general trend is that the glass transition temperature and the gas permeabilities decrease simultaneously with increasing length of the diamine moieties. Polymer structure, T_g , values of permeability for CO_2 and O_2 , as well as values of P_{CO_2}/P_{CH_4} and P_{O_2}/P_{N_2} for the 6FDA-based polyamideimides studied in the present work and the 6FDA-based polyimides studied by Stern *et al.*²¹ are compared in Table 2. Interestingly, the general trend mentioned above is not suited to the polyamideimides when oligo(tetrafluoroethene) segments were introduced into the polymer chain. In fact, with increasing segment length the glass transition temperature was lowered but the permeabilities increased by approximately 1–2×.

Diffusivities and solubilities

Tables 3 and 4 summarize the diffusion coefficients (D), diffusion selectivities ($\alpha_{A/B}^D$), solubility coefficients (S) and solubility selectivities ($\alpha_{A/B}^S$) respectively for various gases at 35°C and 10 atm upstream pressure in the studied polymers. These data show that in a given polymer the diffusion coefficients decrease in the penetrant gas order: $D(O_2) > D(CO_2) > D(N_2) > D(CH_4)$. It is well known that

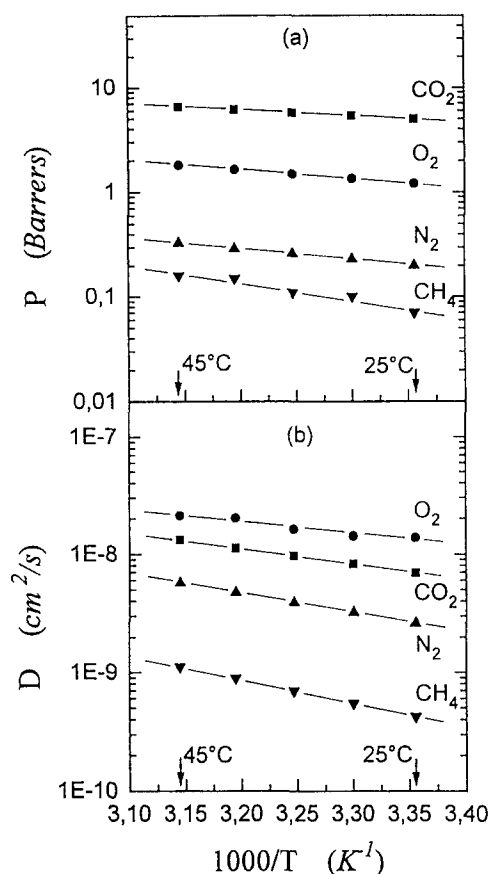


Figure 5 Temperature dependence of (a) permeabilities and (b) diffusivities for 6FDA/8p polyamideimide at 10 atm

the diffusion process is dependent on the size and shape of the molecule. Therefore, a general trend should be that the diffusion coefficients in a given polymer decrease with increasing the kinetic diameter (σ_k) of the penetrant molecules. However, the diffusion coefficients for CO_2 and O_2 obtained in this study depart from this trend because $D(\text{O}_2) > D(\text{CO}_2)$ whereas $\sigma_k(\text{O}_2) > \sigma_k(\text{CO}_2)$ ³⁴. Similar behaviour has also been observed for other types of glassy polymers including polyimides^{7–22}, polycarbonates^{3,4} and polysulfones^{5,6}. These results will be more thoroughly discussed during analysis of the activation energies for diffusion.

Further, data presented in Tables 3 and 4 also show that the higher permeabilities for 6FDA/8p relative to its 6FDA/8m isomer is a result of both its higher diffusivities and solubilities. The diffusivities of CO_2 and O_2 in 6FDA/8p are 100% and 60% greater than those in 6FDA/8m, while the solubilities of CO_2 and O_2 in the former polymer are 70% and 90% larger than those in the later polymer respectively. However, the higher gas permeabilities for the 6FDA/12p membrane relative to the 6FDA/12m are mainly due to the higher solubilities in the *para* isomer. As can be seen from Tables 3 and 4, the diffusivities of CO_2 and O_2 in these two isomers are relatively constant, whereas the solubilities of CO_2 and O_2 in 6FDA/12p are 2.1 and $1.8 \times$ greater than in 6FDA/12m.

Generally, the solubility of a gas is thermodynamic in nature and is determined by: (1) the inherent condensibility of the gas; (2) the polymer–gas interactions; (3) the amount and distribution of excess free volume in the glassy polymers. On the other hand, the diffusion

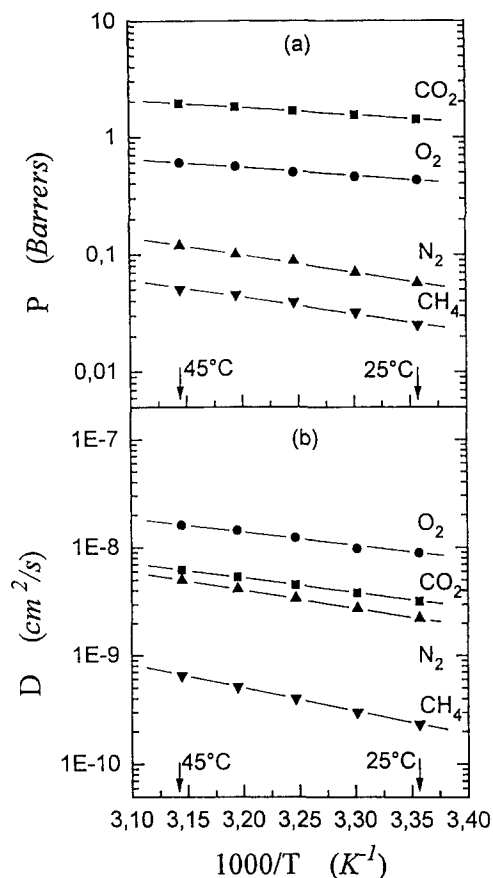


Figure 6 Temperature dependence of (a) permeabilities and (b) diffusivities for 6FDA/8m polyamideimide at 10 atm

coefficient is mainly determined by the chain packing and the mobility of the polymer chain segments as well as the size and shape of the gas molecule¹⁶. In the polymeric membranes studied here, segmental mobility can be increased by using a *para*-connected phenyl group instead of a *meta*-connected one, or by increasing the length of the flexible oligo(tetrafluoroethylene) segment. The diffusivity and solubility results mentioned above may be due to the fact that, comparing with the effect of the flexible oligo(tetrafluoroethylene) segment, the substitution patterns of phenyl group in the diamine moieties have a much lesser effect on the segmental mobility, in turn, on the diffusivities in the 6FDA-polyamideimides as the length of the flexible oligo(tetrafluoroethylene) segment increasing from 8 to 12 carbons.

Further research on the gas transport properties of this kind of polymer with less than 8 and more than 12 carbons of flexible oligo(tetrafluoroethylene) segment in the diamine moieties is necessary to elucidate this hypothesis.

Temperature dependence of transport properties

The effect of temperature on permeabilities and diffusivities for CO_2 , O_2 , N_2 , and CH_4 at 10 atm upstream pressure is presented in Figures 5–8. From these figures it is clear that the temperature dependence of P and D for the four 6FDA-polyamideimides can be described by the Arrhenius equations (6) and (7). As with all other polymers reported in the literature¹⁸, the general trend is that the gas permeabilities and diffusivities increase with temperature.

E_P and E_D as well as P_0 and D_0 obtained from the

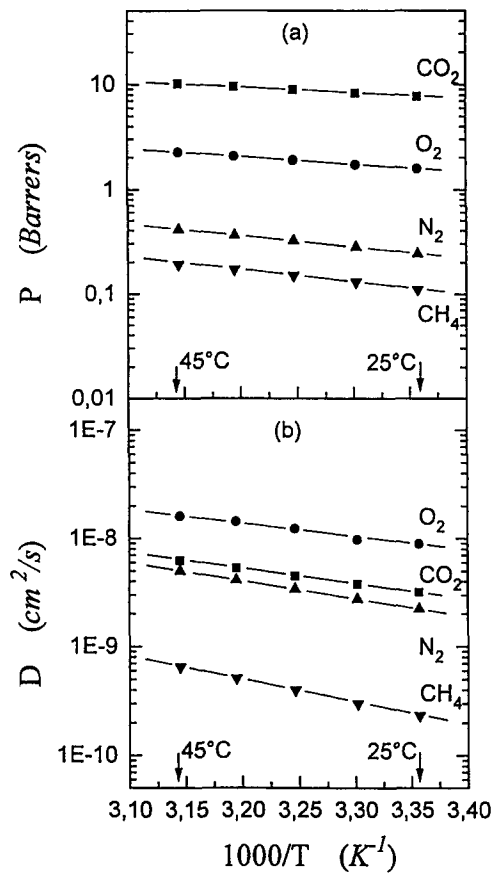


Figure 7 Temperature dependence of (a) permeabilities and (b) diffusivities for 6FDA/12p polyamideimide at 10 atm

Table 5 Activation energies for permeation and diffusion for four penetrants in the 6FDA-polyamideimides

Polymer	6FDA/8p	6FDA/8m	6FDA/12p	6FDA/12m
E_p (kcal mol ⁻¹)				
CO ₂	2.60	2.89	2.46	2.54
O ₂	3.81	4.01	3.30	3.47
N ₂	4.54	5.58	4.04	4.22
CH ₄	5.83	6.37	5.15	5.56
E_D (kcal mol ⁻¹)				
CO ₂	6.02	6.24	5.22	5.66
O ₂	4.91	5.58	4.56	4.90
N ₂	7.27	7.57	6.66	6.93
CH ₄	9.15	9.62	8.70	8.16

Table 6 Pre-exponential factors for four penetrants in the 6FDA-polyamideimides

Polymer	6FDA/8p	6FDA/8m	6FDA/12p	6FDA/12m
$P_0 \times 10^{-2}$ (Barrers)				
CO ₂	3.98	1.86	4.94	2.31
O ₂	7.48	3.46	4.15	2.88
N ₂	4.43	7.47	2.89	1.98
CH ₄	16.04	13.25	7.54	8.20
$D_0 \times 10^3$ (cm ² s ⁻¹)				
CO ₂	0.18	0.12	0.058	0.10
O ₂	0.05	0.094	0.039	0.06
N ₂	0.56	0.79	0.23	0.43
CH ₄	2.15	2.64	1.55	0.70

Arrhenius plots are given in *Tables 5* and *6* respectively. The permeation activation energies reported for the four polyamideimides in *Table 5* follow the same general trends as those reported by other investi-

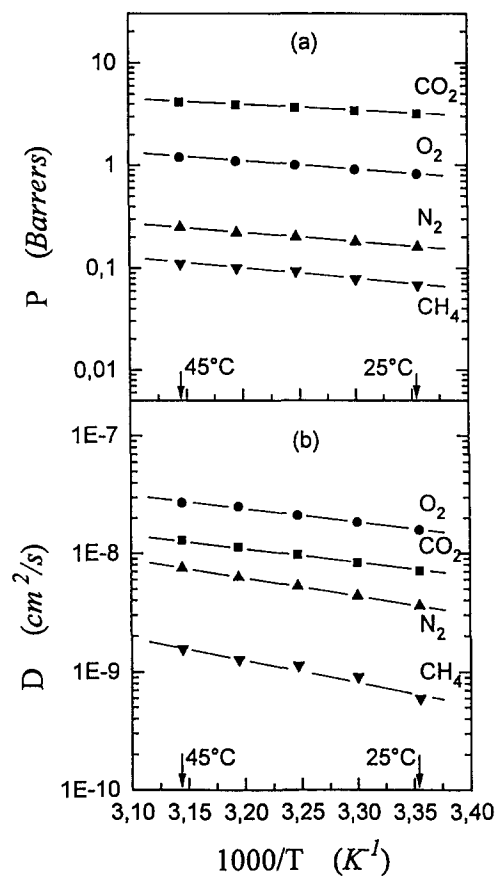


Figure 8 Temperature dependence of (a) permeabilities and (b) diffusivities for 6FDA/12m polyamideimide at 10 atm

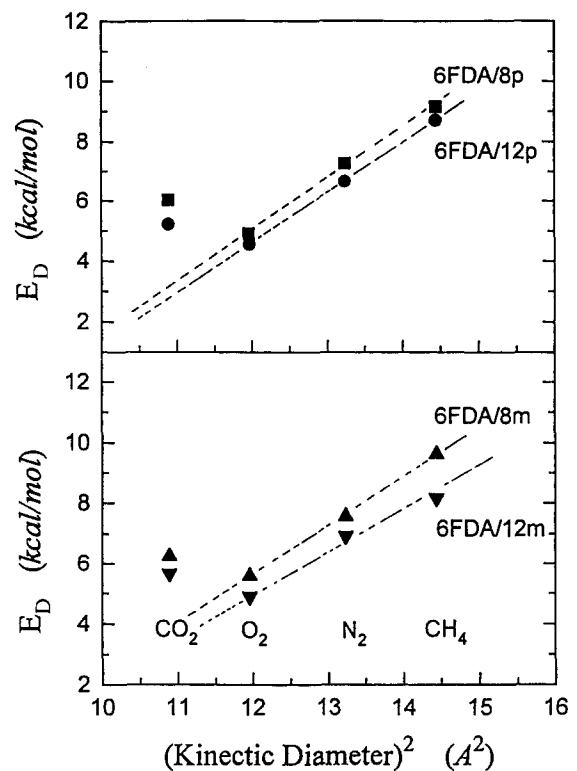


Figure 9 Correlation of activation energies for diffusion with penetrant size

gators^{4,15,21}, that is, E_p increases with penetrant size for each polymer. Meares³⁸ interpreted the diffusion of a penetrant as a process that occurs along a cylindrical volume defined by the penetrant diameter, σ , and the

average length of its diffusion step, λ . According to this interpretation, the activation energy for diffusion and the penetrant diameter should be related by:

$$E_D = \frac{\pi}{4} \cdot \sigma^2 \cdot \lambda \cdot CED \quad (8)$$

where CED is the cohesive energy density of the polymer. Following equation (8), Figure 9 shows the correlation between the E_D values and the square of the kinetic diameters of the gases. It is quite evident that the E_D values for CO_2 are higher than expected. Corresponding to the diffusion coefficients order mentioned in the previous section, the relative magnitudes of E_D for CO_2 and O_2 are anomalous from their diameters also.

A possible cause for the higher diffusivity and lower diffusion activation energy of O_2 compared to those of CO_2 is the strong quadrupole moment of the CO_2 molecule²¹, which may induce specific interactions between CO_2 and the polar groups in the polyamideimides, such as the $-(\text{CF}_2)-$, $-(\text{CF}_3)$ and $\text{C}=\text{O}$ groups in the polymer chain. On the other hand, the O_2 molecule is nonpolar. Stern *et al.*²¹ suggested that the specific CO_2 /polymer interactions may hinder the mobility of the CO_2 molecules in the polymer matrix, and as a result $D(\text{O}_2) > D(\text{CO}_2)$. To activate this hindered mobility, more energy should be needed, thus, $E_D(\text{CO}_2) > E_D(\text{O}_2)$. Another possible reason for the anomalies mentioned above is the difficulty in estimating an accurate diameter of CO_2 molecule because of its nonspherical nature. Stern *et al.*²¹ suggested that the CO_2 molecule may have a larger effective size, possibly between its kinetic diameter of 3.3 Å and its collision diameter of 3.94 Å.

ACKNOWLEDGEMENTS

One of the authors, Dr Zhikang Xu, is thankful to Zentrum für Technologische Zusammenarbeit of TU Berlin for a fellowship. Useful suggestions and help of Dr Bihai Song and Mr Gonghao Chen are also acknowledged.

Parts of the work were also supported by the Max-Buchner-Forschungstiftung.

REFERENCES

- 1 Kesting, R. E. and Fritzsche, A. K. 'Polymeric Gas Separation Membranes', John Wiley, New York, 1993
- 2 Paul, D. R. and Yampol'skii, Yu. P. (Eds) 'Polymeric Gas Separation Membranes', CRC Press, New York, 1994
- 3 Schimidhauser, J. C. and Longley, K. L. *J. Appl. Polym. Sci.* 1991, **39**, 2083
- 4 Costello, L. M. and Koros, W. J. *J. Polym. Sci., Polym. Phys. Edn* 1994, **32**, 701
- 5 McHattie, J. S., Koros, W. J. and Paul, D. R. *Polymer* 1991, **32**, 840
- 6 Aitken, C. L., Koros, W. J. and Paul, D. R. *Macromolecules* 1992, **25**, 3425
- 7 Sykes, G. F. and St. Clair, A. K. *J. Appl. Polym. Sci.* 1986, **32**, 3725
- 8 Kim, T. H., Koros, W. J., Husk, G. R. and O'Brien, K. C. *J. Membr. Sci.* 1988, **37**, 45
- 9 Stern, S. A., Mi, Y., Yamamoto, H. and St. Clair, A. K. *J. Polym. Sci., Polym. Phys. Edn* 1989, **27**, 1887
- 10 Mi, Y., Stern, S. A. and Trohalaki, S. *J. Membr. Sci.* 1993, **77**, 41
- 11 Tanaka, K., Okano, M., Toshino, H., Kita, H. and Okamoto, K. *J. Polym. Sci., Polym. Phys. Edn* 1992, **30**, 907
- 12 Matsumoto, K., Xu, P. and Nishikimi, T. *J. Membr. Sci.* 1993, **81**, 15
- 13 Langsam, M. and Burgoyne, W. F. *J. Polym. Sci., Polym. Chem. Edn* 1993, **31**, 909
- 14 Tanaka, K., Kita, H., Okano, M. and Okamoto, K. *Polymer* 1992, **33**, 585
- 15 Costello, L. M. and Koros, W. J. *J. Polym. Sci., Polym. Phys. Edn* 1995, **33**, 135
- 16 Coleman, M. R. and Koros, W. J. *J. Polym. Sci., Polym. Phys. Edn* 1994, **32**, 1915
- 17 Coleman, M. R. and Koros, W. J. *J. Membr. Sci.* 1990, **50**, 285
- 18 Matsumoto, K. and Xu, P. *J. Appl. Polym. Sci.* 1993, **47**, 1961
- 19 Coleman, M. R., Kohn, R. and Koros, W. J. *J. Appl. Polym. Sci.* 1993, **50**, 1059
- 20 Zoia, G., Stern, S. A., St. Clair, A. K. and Pratt, J. R. *J. Polym. Sci., Polym. Phys. Edn* 1994, **32**, 53
- 21 Stern, S. A., Liu, Y. and Feld, W. A. *J. Polym. Sci., Polym. Phys. Edn* 1993, **31**, 939
- 22 Glatz, F. P., Mülhaupt, R., Schultze, J. D. and Springer, J. *J. Membr. Sci.* 1994, **90**, 151
- 23 Steinhäuser, N., Mülhaupt, R., Hohmann, M. and Springer, J. *Polym. Adv. Technol.* 1994, **5**, 438
- 24 Aguilar-Vega, M. and Paul, D. R. *J. Polym. Sci., Polym. Phys. Edn* 1993, **31**, 1577
- 25 Bourbon, D., Kamiya, Y., Mizoguchi, K. *J. Polym. Sci., Polym. Phys. Edn* 1990, **28**, 2057
- 26 Xu, Z.-K., Böhning, M., Schultze, J. D., Li, G. -T., Springer, J., Glatz, F. P. and Mülhaupt, R. *Polymer* submitted
- 27 Schultze, J. D. PhD. Thesis, Technische Universität Berlin, D83, Verlag Shaker, Aachen, 1992
- 28 Schultze, J. D., Böhning, M. and Springer, J. *Macromol. Chem* 1993, **194**, 431
- 29 Crank, J. 'The Mathematics of Diffusion', 2nd Edn, Oxford University Press, Oxford, 1975
- 30 Frisch, H. L., Stern, S. A. *CRC Crit. Revs: Solid State Mater. Sci.* 1983, **11**, 123
- 31 Stannett, V. T. in 'Diffusion in Polymers' (Eds J. Crank and G. S. Park), Academic Press, London, 1968
- 32 Stannett, V. T. 'Diffusion in Polymers', John Wiley, New York, 1971
- 33 Engelmänn, I. Ph.D. Thesis, Technische Universität Berlin, D83 Verlag Shaker, Aachen, 1993
- 34 Breck, D. W. 'Zeolite Molecular Sieves', John Wiley, New York, 1974, Chapter 8
- 35 Light, R. R. and Seymour, R. W. *Polym. Eng. Sci.* 1982, **22**, 229
- 36 Scheu, F. R. and Chern, R. T. *J. Polym. Sci., Polym. Phys. Edn* 1989, **27**, 1121
- 37 Pavlova, S. S. A., Timofeeva, G. I. and Ronova, I. A. *J. Polym. Sci., Polym. Phys. Edn* 1980, **18**, 1175
- 38 Meares, P. *J. Am. Chem. Soc.* 1954, **76**, 3415